TECHNICAL TRANSACTIONS | **CZASOPISMO TECHNICZNE**
ELECTRICAL ENGINEERING | ELEKTROTECHNIKA

2-E/2015

JERZY SZCZEPANIK*, TOMASZ SIEŃKO*

MICROPROCESSOR CONTROLLED MATRIX CONVERTER CONNECTOR FOR POWER SYSTEMS

STEROWANY MIKROPROCESOROWO PRZEKSZTAŁTNIK MACIERZOWY DO APLIKACJI W SYSTEMACH ELEKTROENERGETYCZNYCH

Abstract

A matrix *N*×*M* multiphase converter is a simple structure incorporating *N*×*M* bi-directional switches, connecting *N* input phases to *M* output phases and able to convert input voltages into output voltages of any shape and frequency. However, commutation problems and complicated control algorithms keep it from being utilized on a large scale. This paper gives a solution to the control system of the multiphase matrix converters for power system application. The practical application of multiphase matrix converters (MC) in power systems involves the study of application requirements, possible converter topologies and the development of new, reliable control algorithms. The MC is working as a connection device between power systems or as an interconnection device within the power system. The proposed tasks performed by the MC in the power system are power flow control and power flow oscillation dumping. The device can be viewed as new FACTS device-series power system connector, based on straightforward energy conversion.

Keywords: *Area Based Control*, *Matrix Converter Control*, *Multiphase Matrix Converter*

Streszczenie

Wielofazowy przekształtnik macierzowy *N*×*M* jest stosunkowo prostą strukturą złożoną z *N*×*M* dwubiegunowych zaworów łączących *N* faz wejściowych z *M* fazami wyjściowymi. Struktura ta teoretycznie może przekształcić dowolne napięcia wejściowe w dowolne napięcie wyjściowe (np. o innej fazie lub częstotliwości). Niestety problemy komutacyjne oraz trudne do implementacji algorytmy sterowania ograniczają możliwość stosowania tego urządzenia. Artykuł przedstawia nową metodę sterowania oraz sposób jej implementacji na mikroprocesor dla wielofazowego przekształtnika macierzowego. Metoda ta jest oparta na sterowaniu obszarowym i przeznaczona do zastosowania w systemie elektroenergetycznym. Praktyczna aplikacja przekształtnika musi w takim wypadku uwzględniać ograniczenia narzucane przez ten system, a wynikające z jego charakteru. Badania obejmują zatem stworzenie nowej procedury sterowania przekształtnika oraz analizę jego pracy w charakterze przesuwnika fazowego z uwzględnieniem narzuconych ograniczeń. Proponowane funkcje przekształtnika to kontrola rozpływu mocy czynnej w systemie oraz zastosowanie przekształtnika w urządzeniach typu FACTS.

Słowa kluczowe: *sterowanie obszarowe*, *sterowanie przekształtnikiem macierzowym*, *wielofazowy przekształtnik macierzowy*

DOI: 10.4467/2353737XCT.15.091.3923

* Ph.D. Eng. Jerzy Szczepanik, Eng. M.Sc. Tomasz Sieńko, Institute of Electromechanical Energy Conversion, Faculty of Electrical and Computer Engineering, Cracow University of Technology.

1. Introduction

FACTS technology is very promising for the power system control. In this paper, a new FACTS unit based on a matrix converter is investigated. Figure 1 shows a schematic diagram of a proposed controller, which consists of two power transformers and a matrix converter installed between them. Power transformers have 3-phase high voltage windings and N-phase windings connected to the $N \times N$ matrix converter (MC). Such a controller has three phase input and output, but energy transfer occurs in an N-phase system. The structures of the proposed devices incorporate transformers on both sides of the converter, this is determined by the necessity to decrease voltage levels to the power electronic equipment requirements and output voltage level control. The MC in this application is not used for voltage level regulation and only frequency and phase of the output is controlled. The simulations of such devices have already been done and reported in the previous authors' papers [1, 2].

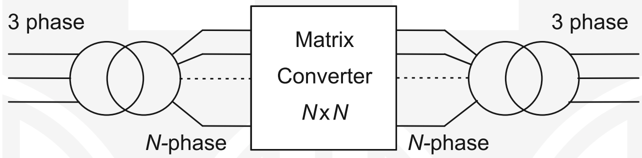

Fig. 1. A diagram of a voltage phase controller

The proposed field of application is a power system. This environment determines several requirements which have to be fulfilled in order to assure the proper operation of the MC based converter as an interconnection device. The MC converter based device has to 'produce' sinusoidal voltages as it works between two voltage sources with relatively low internal impedances (in conventional machine drive applications, sinusoidal currents are required [3–17]) and control (adapt) phases and frequencies on both sides of the apparatus. Such a device can control network power flow by shifting the phase of its output voltage, this results in changes of active power flow via network branches. Several other requirements such as continuous current flow, low contents of low order harmonics and lack of short circuits on both sides of the converter were taken into consideration during the device development. The PWM (pulse with modulation) switching strategies were not utilized in power system applications due to high power transfer, relatively large switching losses and control problems during their operation. Thus, in the proposed application, the MC works as a device that creates output voltage as a combination of the input voltages.

Multiphase (more than three phase) MC structures [18–23] were investigated as more promising for the proposed application due to the bad performance of the previously researched three phase systems. This bad performance of 3×3 structures means, in real life applications, a low and angle shift dependent voltage transfer, a high content of low order harmonics in converter voltages and currents [24–26], and the necessity to transfer entire power (at a given instant) through a maximum of only three switches (a minimum of two have to be open to assure current flow).

The main task of this research is to develop a multiphase MC based power system link characterized by a much better performance than the three phase version. The crucial part of the project was the development of the control strategy most suitable for a proposed application and then the design of the control algorithm which can be applied in the real life digital controller. In order to produce sinusoidal voltages, the investigated strategies have to utilize all available values of input voltages, thus, they create outputs not only from fragments of the voltages lying at the envelope of the input voltages (as PWM based techniques) but they also use intermediate input voltage values.

2. The Development of The MC Control Algorithm

In the proposed field of application, the MC is a device which creates output voltage as a combination of the input voltages. Thus, for the multiphase MC structure, the first intuitive approach to the control system is to build the output voltage for a chosen output phase at a certain instant from the input phase, which voltage is at this instant closest to the desired one (the 'as close as possible' approach). The second option is to create output voltage from part of the certain input phase in the neighborhood of the point at which this input phase crosses the desired output waveform (the 'crossing point' approach). These algorithms are easy to build as an analog control system and can be easily simulated using for example, Matlab programming. The algorithm at a certain instant simply compares all input phases to the desired output waveform, chooses the input which is the closest and switches on the switch between the output and this chosen phase. Thus, in theory, the algorithm can be used to create with a certain adequacy, any shape of output from any waveforms of the input.

In this research, and for a proposed application, the shapes of waveforms are close to sinusoids, both at the input and at the output. For the 'as close as possible' algorithm, the switches are not turned 'on' for the same period of time, but the advantage of this strategy appears when the intervention of the MC is not required. Then, the desired output is equal to the input and there is no switching necessary – input phases are connected straight to the output. For switching strategy 'around crossing point' the switching periods are constant and, for example, for a 12×12 MC structure, they last for the time equivalent of 15 degrees. Thus, the switching algorithm can be simplified and the parameters of the output are constant – voltage transfer, *THD* and phase shift between the applied one and the phase of the first harmonic of the output.

The algorithms constructed in the proposed way do not guarantee to satisfy all requirements of the application, for example, short circuits are excluded. Several simulations were completed to research properties of the MC working under proposed controls. It can be noticed that the second approach can be considered as a special case of the first one for a certain phase shift between input and output waveforms. The waveforms obtained from analog simulation are shown in Figs. 2 and 3.

It is visible that the output waveform of the MC becomes closer to the desired one as the number of input phases increases (Fig. 2). The structures incorporating 6×6, 12×12 and 12×3 matrix of the switches were investigated in this research due to the fact that the six and twelve phase transformers are already on the market and they are used in power systems, for example, in DC link applications. The structure of the 12×12 MC incorporates 144 two-way switches, this was considered as a maximum due to the cost of the device.

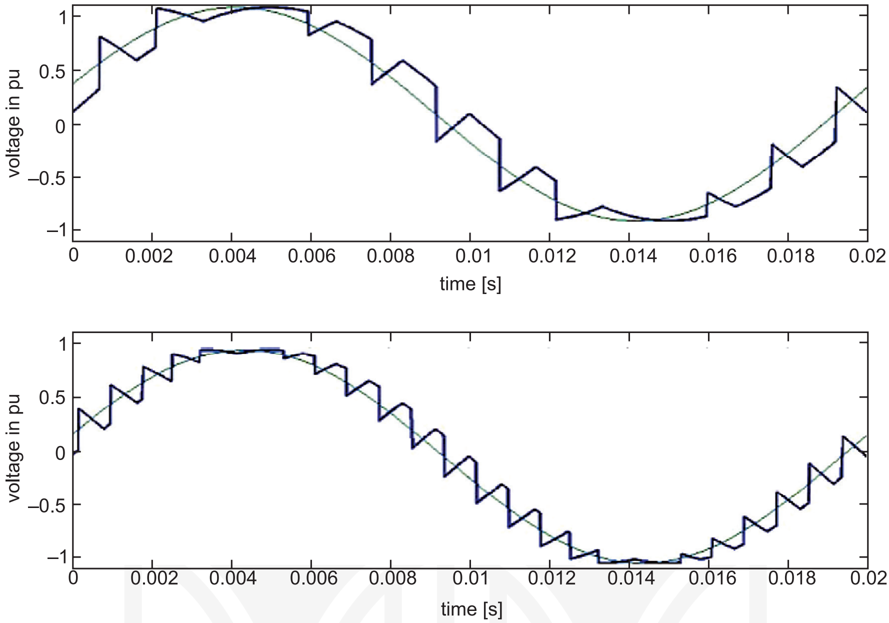

Fig. 2. Output waveform of the 6×6 (upper figure) and 12×12 MC (lower figure) under proposed 'as close as possible' control approach for 50 Hz to 50 Hz conversion and phase shift

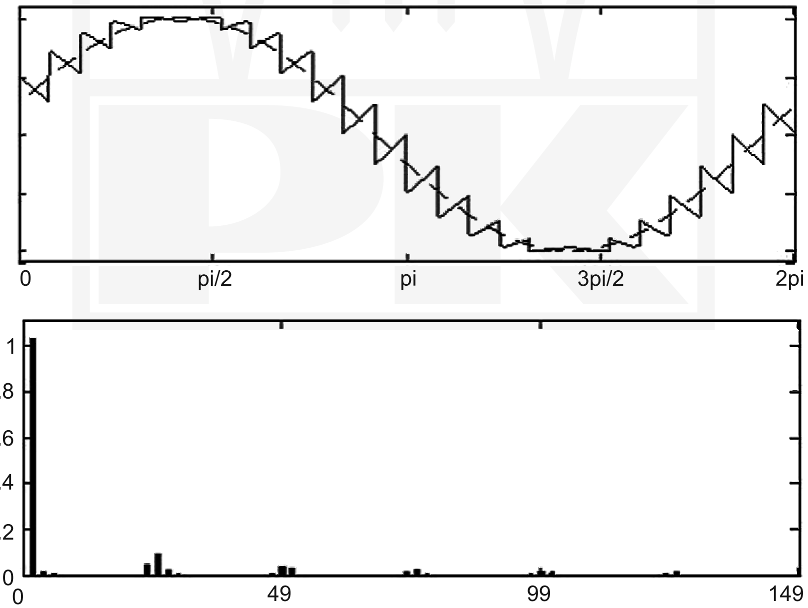

Fig. 3. Output waveform of the 12×12 MC under proposed 'crossing point' control approach versus the desired sinusoidal waveform (upper figure) and it's FFT (lower figure)

The proposed control strategies can be viewed as similar to the multilevel converter control strategies. It can be also noted that for input frequencies higher than 50 Hz, the adequacy of the desired waveform approximation by the MC converter increases. It can be simply explained by the fact that during the whole period of the 50 Hz output, there are more possibilities to find input waveforms close to the desired output waveform. This property of the MC working under the proposed control makes it suitable for the connection of the high frequency generators to the grid.

Properties of the investigated control algorithm are very promising – Fig. 3 shows the 12×12 MC output voltage waveform and its FFT for the second control approach, which is the worst distortion case for the 'as close as possible' approach. The converter currents and voltages are showing small harmonic distortions and contain only high order harmonics, which are easy to filter.

Due to the fact that in real life, it is impossible to implement the proposed control schemes using the digital controller and not all requirements are satisfied, the research led to developing a correlation of algorithms with already known ones which are easily applicable for a multiphase MC. The vector control strategy and the 'area' based control scheme was found to be the most promising in the digital controller application.

3. The 'area' Based Control Scheme For a Multiphase MC

In general, the output voltage for every output phase of the MC can be written as:

$$V_{\text{out}}(t) = G_1(t) \cdot V_1(t) + G_2(t) \cdot V_2(t) + \ldots + G_n(t) \cdot V_n(t) \tag{1}$$

where:

$G_n(t)$ – membership function for a given output phase and n-th input phase,
$V_n(t)$ – voltage for the n-th input phase.

The $G_n(t)$ membership function specifies at which time instant and for how long a certain m-th output phase voltage consists of the n-th input phase voltage. During the interval, when output voltage consists of a fragment of the n-th input voltage, the $G_n(t)$ function achieves the value '1' and in the other cases, its value equals '0' (Fig. 4).

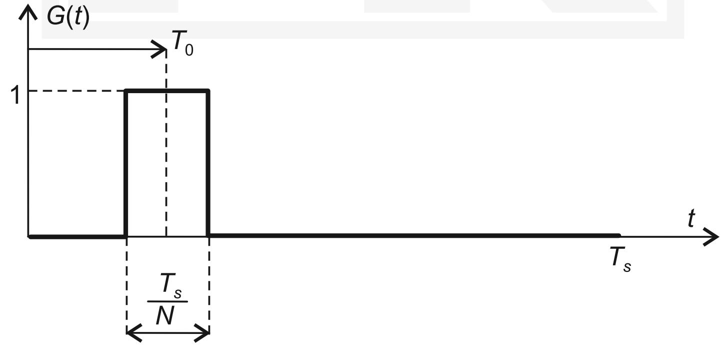

Fig. 4. An example basic membership function

In fact, the membership function specifies the MC control strategy and the shape of the output voltage waveform to be obtained. All existing control strategies can be expressed as a search for the specific membership function. Of course, if the MC creates output voltages from fragments of input ones, it also introduces ties to its input and output currents. Then the relation of all input quantities (voltages and currents) and output ones can be stated as [27, 28]:

$$\begin{bmatrix} V_N \\ I_M \end{bmatrix} = \begin{bmatrix} G & 0 \\ 0 & G^T \end{bmatrix} \begin{bmatrix} V_M \\ I_N \end{bmatrix} \tag{2}$$

where G is matrix of a membership functions.

The control algorithm used in this research adopted the so-called ‘area’ approach described in [29, 30]. This control strategy is based on a geometrical interpretation of functions describing actual state of the MC switches, since the shape of the membership function depends on the relative position of a certain input phase with respect to the desired output. Thus, the membership function can be viewed as a function of input and output voltage running phases where time is a parameter and all control processes can be analyzed in a two-dimensional space. For every switch (valve) in the MC structure, the state of this device can be determined at any instant on the plane where the value of the coordinate on the X axis is the value running phase of the input at this instant, and similarly, the Y axis represents the running phase at the output. Time is a parameter determining the values of the running phases, thus any time instant is represented by a unique point on the plane. If the running phases are continuous functions of time, the points determined on the plane by running phases (coordinates) are forming, as time elapses, a continuous curve. This curve is called the trajectory. When input and output frequencies are constant and running phases are linear functions of time (as in considered control scheme for sinusoidal waveforms), then the trajectory is a linear function in the considered space:

$$y = \frac{\omega_1}{\omega_2} x + \varphi \tag{3}$$

where φ is an initial angle difference between input and output.

If input and output waveforms are periodical, then the plane over which the membership function is defined can be limited to the rectangle of the size one period by one period.

When frequencies are different at the input and output, as time elapses, the running phase of higher frequency achieves the full period first then phase of lower frequency and at this point, phase of higher frequency is shifted to ‘0’ (equivalent of repetition sequence in the second period). Thus, in such a space when any one of the input or output running phases reaches the border of this space, the trajectory is shifted to 0 (Fig. 5).

For the proposed application, the input and output waveforms of the MC are sinusoidal, thus, the proposed control space is limited to the square $((0, 2\pi) \times (0, 2\pi))$ which corresponds to the 360 degrees by 360 degrees square. Since the state of the switch is regarded as a function of running phases, it can be observed that inside the control space, the points representing the ‘on’ state are forming a certain area over which the membership function obtains the value ‘1’. This area is called the conduction area and it is attached to a certain single switch. If the trajectory, determining the relative position of the input and output waveforms, has common points with this area, that switch is in the 'on' state. Otherwise, the switch is in the 'off' position. Please note that due to the long time period of the research and different requirements of the simulation and controller software, running phases of the input and output waveforms are given in radians or degrees.

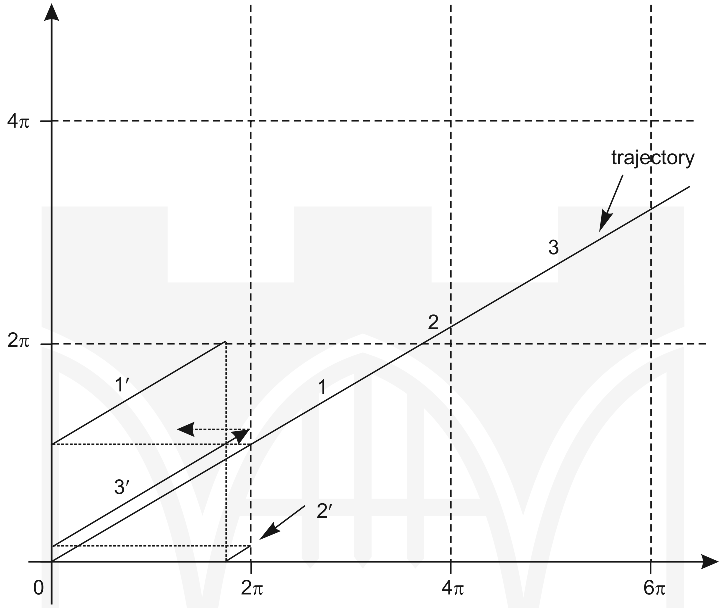

Fig. 5. Reduction of the trajectory into ((0, 2π) × (0, 2π)) subspace for periodical sinusoidal waveforms

In such an approach, the position and the shape of the area in control space determines when and how long the switch will be open, thus, it determines the switch control strategy. The advantage of the proposed approach is that the shape of the conduction area is independent of frequency and initial phase shifts of input and output waveforms. The proposed control scheme requires one and only one control space together with the conduction area for every switch, thus for $N \times M$ MC structure, the generation of $N \times M$ control spaces is required.

It can be noted that for the considered strategy of the conversion, the output waveform is created from parts of the input waveforms which are close to the waveform crossing. For two sinusoidal waveforms, the given waveform and the desired waveform, both with the same amplitude, the determination of the waveform crossing point can be done by solving a simple equation:

$$\sin \vartheta_1 = \sin \vartheta_2 \tag{4}$$

where:

ϑ_1, ϑ_2 – running phases of the input and output waveforms.

The solution is:

$$\vartheta_1 = \vartheta_2 + 2k\pi \quad \text{or} \quad \vartheta_1 = \pi - \vartheta_2 + 2k\pi \tag{5}$$

where $k \in C$.

In the proposed control space, the graphic interpretation of the above equations create the following diagram (Fig. 6).

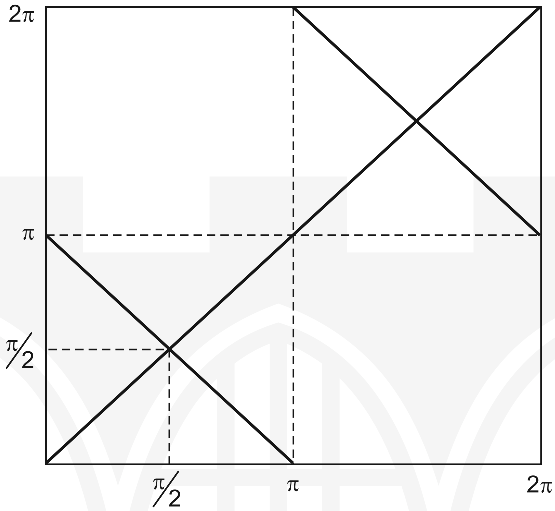

Fig. 6. Diagram corresponding to the solution of the equation (8)

These divagations can be repeated for all *N* input phases. What changes for the *n*-th input is the argument (running phase) of the first sinusoidal function in formula (4) which results in the following statement:

$$\sin(\vartheta_1 - 2\pi n / N) = \sin \vartheta_2 \tag{6}$$

Its solution is similar as in the case of the first phase and it is shifted along the X axis by $2\pi \cdot n/N$.

The conduction areas for the 'as close as possible' approach for the first switch have to lay in the vicinity of the lines from Fig. 6 since these lines represent the crossing points of the sinusoidal waveforms. The shapes of the conduction areas are, in theory, arbitrary, but if the input and output voltages assume the form of sinusoidal functions with the mean value during the period equal to zero (zero offset), the conduction areas for every switch have to be shaped according to the following rules [31]:

– They have to have the same shape for every switch which assures symmetry in every phase.
– The area corresponding to the conduction area of the first switch (G_{11}) is symmetrical in relation to the diagonals of the ((0,2π) × (0,2π)) space, this allows the creation of a symmetrical waveform (Fig. 6).

– For N input and M output phases, the following conduction areas are obtained by repeatedly shifting the base conduction area (G_{11}) by $2\pi/N$ along the X axis and by $2\pi/M$ along the Y axis ($N \times M$ switches).
– To avoid a short-circuit at the input, any cross-section of every conduction area along the X axis cannot be longer than $2\pi/N$, since if conduction areas which are used to drive switches connected to a certain output phase do not have common points, there are no short circuits caused by these switches between the input terminals. The same statement can be derived for the output terminals of the MC.
– Any cross-section of every conduction area along the Y axis cannot be longer than $2\pi/M$ to avoid a short-circuit at the output.
– Another stated condition is that $N \times M$ – this means that the number of input phases is equal to or greater than the number of output phases.
– For square structures ($N \times N$), if the sum of the conduction areas associated to one input or one output phase covers all $((0,2\pi) \times (0,2\pi))$ space, then the current of this phase is continuous which means that this phase is always connected respectively to the output or input phase.

For any MC structure, the control space should be covered by the conduction areas minimum two times at every point, which corresponds to minimum two switches turned 'on'. This condition is necessary to allow the current flow through MC when the structure without the neutral conductor is used.

The generations of the areas for the 'as close as possible' approach were conducted using an analog control algorithm by performing 360 simulations and increasing the phase shift between the input and output waveforms every one degree for every following

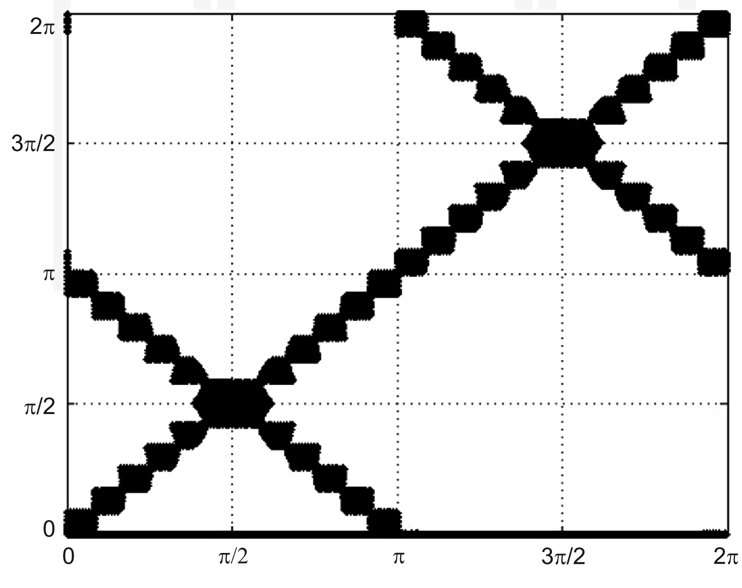

Fig. 7. Conduction areas generated from the intuitive control approach for the application in 'area' based algorithm for a switch 11 (switch between first output and first input phase)

simulation. The parts of trajectories along which the function F achieves the value '1' belong to the conductions areas. The generated conduction areas for a 12×12 structure are shown in Fig. 7. Of course, the layout of the generated areas is the same as the layout of lines representing the solution to equation (7) and it is shown in Fig. 6, since the points along these lines represent the situation when the output is equal to the input.

A similar generation procedure can be performed for the earlier described 'crossing point' approach or for the 'two closest' approach where the output sinusoidal waveform is created from two closest to it input waveforms [32].

The conduction areas similar to the one from Fig. 7 allow generating an output voltage waveform as a combination of the 'closest' parts of the input voltages sinusoids using the 'area' based approach. However, this control scheme does not satisfy all previously stated conditions required from the MC in the power system application, thus, the conduction areas had to be modified (Figs. 8–10).

The conduction areas for every switch are created from a basic structure obtained for a G_{11} switch by shifting the structure in the Y and X direction by the multiplication of the switch index and π/N.

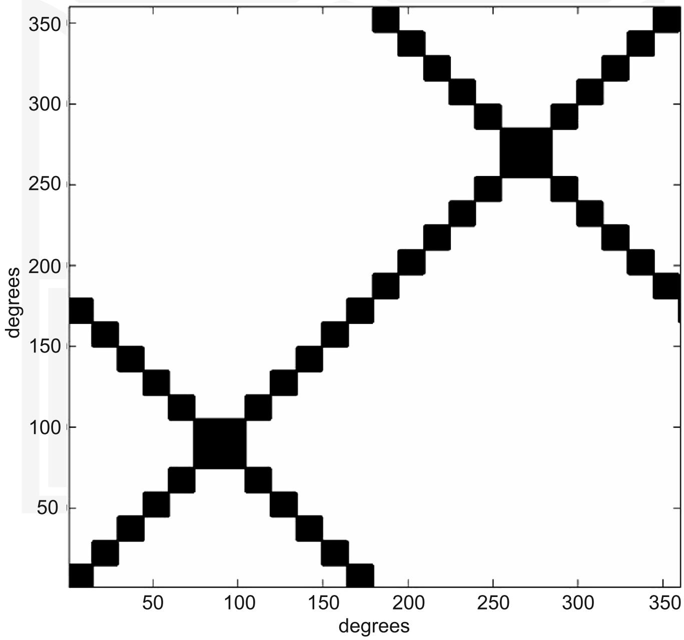

Fig. 8. G_{11} conduction area applied to the 'area' based MC control algorithm created on the basis of the areas from Fig. 4 and on the basis of the stated conditions

Figure 9 shows the shape of the conduction area for the 'crossing point' approach [33–36].

The performances of the proposed MC control schemes were investigated using Matlab Simulink software. A matrix lattice was build using a standard switch from SimPowerSystems library – source, loads and measuring blocks are standard Simulink blocks.

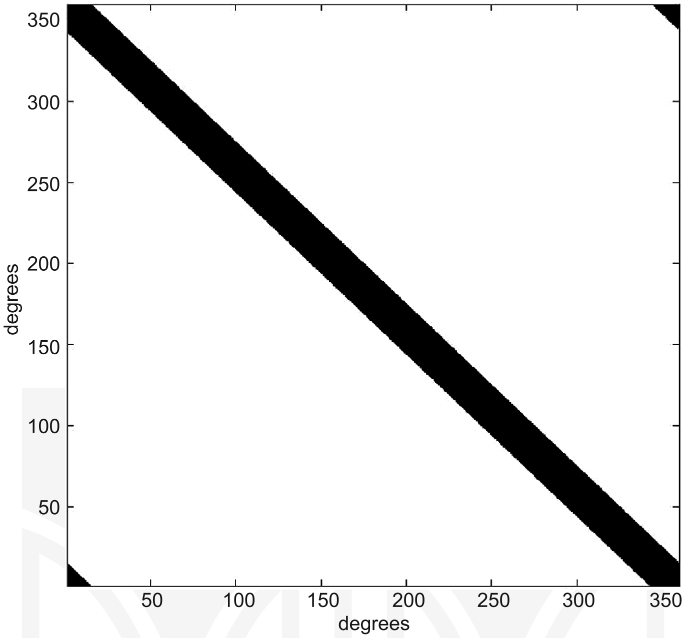

Fig. 9. Basic G_{11} conduction area for a crossing point approach

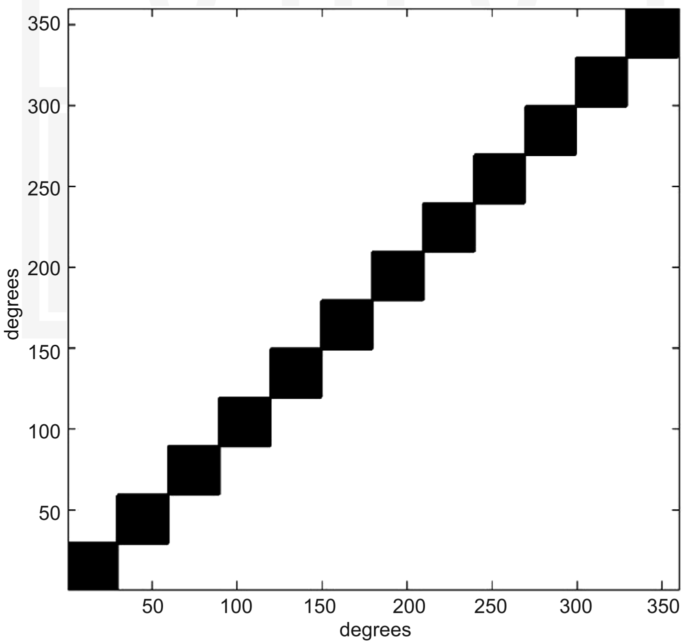

Fig. 10. Basic G_{11} conduction area for a two closest approach

The conduction areas for the proposed control scheme were generated assuming one degree resolution, using the developed software in the form of 360×360×144 matrix stored in the Matlab workspace. Each 360×360 layer of this matrix represents the conduction areas for a specific switch. The conduction areas are grouped in 12 layer structures, each representing conduction areas of row or column of MC switch lattice.

At a certain instant, the position of the point on the trajectory (its coordinates) representing phases of the input and output voltage at this instant, is compared with the layout of the conduction areas in every layer. If this point is situated inside the conduction area at a certain layer, the switch represented by this layer assumes the 'on' state.

This technique can be easy adapted for a digital control as a direct memory search technique for earlier generated conduction areas. The control algorithm for the purpose of the simulation has been written as a Matlab's *S*-function, where inputs are input and output frequencies, phase shift and simulation time. The 360×360×144 matrix of the conduction areas is implemented as a constant parameter of the *S*-function. The output of the *S*-function is a 144 column vector representing the states of all the switches – '0' is equal to the 'off' state and '1' is equal to the 'on' state of the switch.

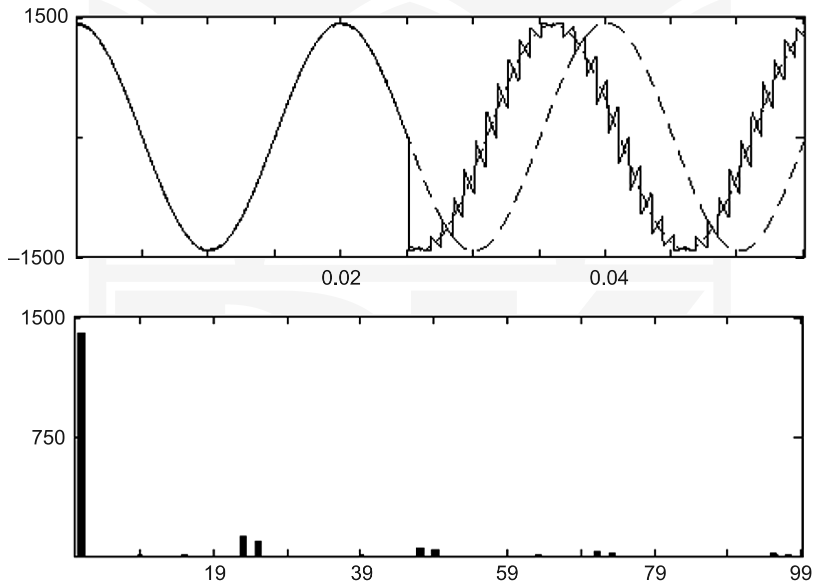

Fig. 11. The output voltage of the 12×12 MC at instant $t = 0.25$ s phase shift 75 degrees was applied and its *FFT* (dash line – waveform of first phase input, dash-dot line first harmonic output waveform)

The simulations of the proposed structure were done for the constant input voltages and constant load values. For the initial simulations, only a symmetrical supply of frequency being a multiple of output frequency and symmetrical loads were considered. This limitation was included only because in the other cases, the results are not so easy to interpret.

4. The Development of the Real Life MC Control System

The control algorithm is usually performed by the microprocessor controller. The proposed algorithm was chosen among the others due to the fact that it is easily applicable to digital control. The ((0,2π) × (0,2π)) planes with conduction areas can be easily generated for a chosen control strategy and a given number of switches in the MC lattice (one plane for one switch). Every plane can be divided into cells with a certain accuracy. For example, the accuracy of one degree can be achieved by dividing each plane to 360×360 cells. The value of membership function over each cell is '0' or '1', thus, one bit is enough to describe the membership function in each cell. Thus, the function over each plane is represented by 360×360×1 bit = 129 600 bits, which equals 16 200 bytes.

For a 12×12 MC structure, the 144 planes have to be generated, thus, the memory required to store all planes has to be greater than 2.2 MB. If the frequency at the output is close to 50 Hz, the required accuracy determines the frequency of switching. For 1° accuracy, the value of the membership function has to be updated every $\Delta t = 55\cdot10^{-6}$ s, which corresponds to 50×360 = 18 kHz switching frequency. The term 'switching frequency' does not determine the change of the switch state, but denotes that at every time interval Δt, the processor base controller has to find a new set of 144 values determining the states of switches and shifts them simultaneously to the output. Of course, the state of the specific switch changes, if the trajectory enters or leaves the conduction area.

Due to the special memory arrangement, the required operations performed in Δt time interval consist of memory cell address calculation from time and trajectory equation and the memory reading from the chosen cell (each cell consists of 18 bytes = 144 bits). For

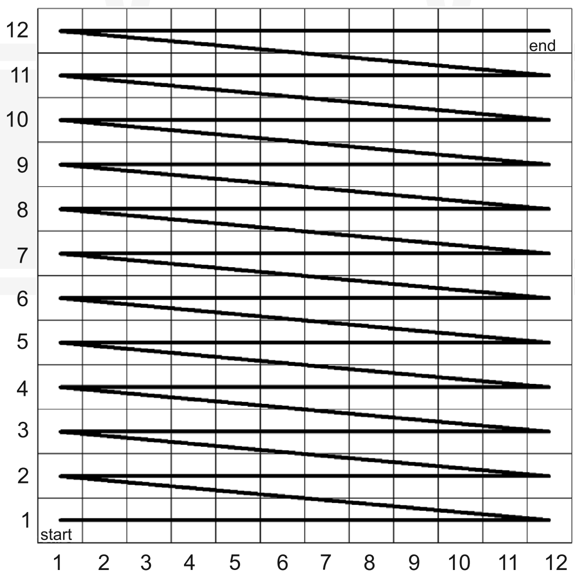

Fig. 12. The decomposition of the three dimensional (360×360×144) matrix into the two--dimensional and memory write procedure

MC lattices smaller then 12×12 – for example for 6×6 structures – only the first 36 bits form each memory cell are filled and the rest is topped by zeros to fill all 144 bits. Then, only the first 36 outputs are taken into consideration and the rest is ignored. This approach allows the development of only one memory search program for every size of the MC lattice (in the case of this research, the size is limited to 12×12 lattice). The zero crossing detectors are necessary to synchronize input and output voltages with trajectory and to determine the frequencies at both sides.

The processor used is a 128 MHz 32 bit device, so for a chosen switch update timing, it uses less than 1/4 of Δt time period to perform the memory search procedure, thus, it is possible to digitize $((0,2\pi) \times (0,2\pi))$ space two times denser in each direction to 720×720 cells. The work of the built controller is shown in Figs. 13 to 14. For the 6×6 structure, 50 Hz to 50 Hz conversion and 15 degrees of the phase shift of the output phase with respect to the input phase, the trajectory (Fig. 13) is delayed with respect to the input phase by 15 degrees. Then, the shape of the membership function of the first input phase in the first output phase is shown in Fig. 13 by a dotted line.

In the real application of the controller, the main problem is the zero sensing procedure and the delay caused by this procedure. The problem of the position of zero voltage becomes a serious problem especially for distorted input voltages (multiple zero crossing, not the same time period between following zero crossing points). The delay caused by the zero sensing procedure was investigated and was found to be the same for every measurement for the same procedure, thus, the correction is not an issue.

Laboratory model of MC was built as 6×6 structure using 36 bi-directional switches built using single IGBT and four diodes structure (Fig. 15).

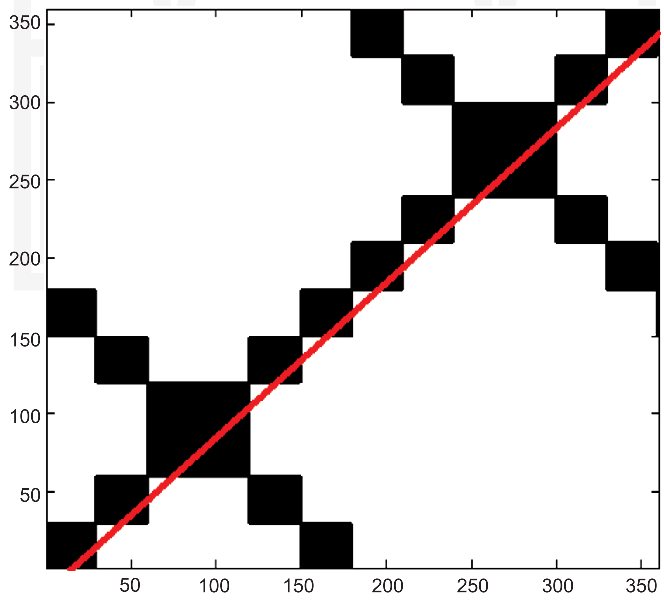

Fig. 13. Trajectory in the G_{11} control plane – the desired phase shift is 15 degrees

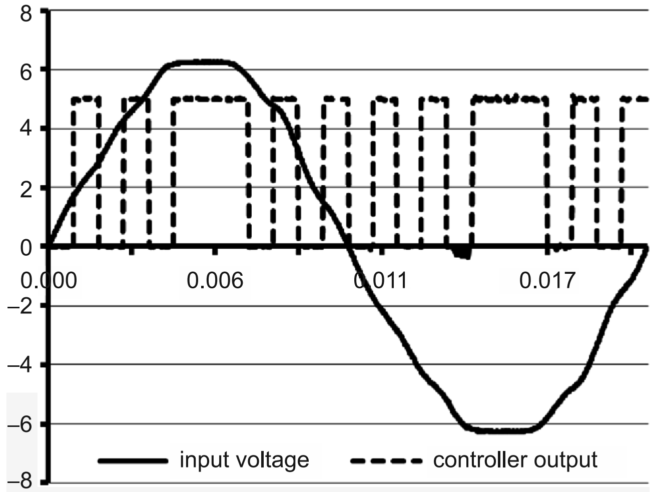

Fig. 14. The membership function for the G_{11} switch versus the voltage of the first input phase for the 15 degrees phase shift – real life measurement – *X* axle – time in [s], *Y* axle – voltage [V]

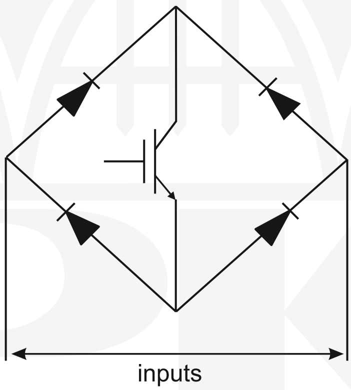

Fig. 15. Structure utilizing single IGBT transistor and four diodes

The advantage of this switch setup includes the usage of a single switching element which requires the generation of only one control signal to fully control the switch current and some properties during commutation. These properties include the possibility of selection diodes with switching times slightly longer than IGBT what reduces diodes switching losses.

The six phase transformers were built using three toroidal three winding transformers for each side of the converter. The primary windings arrangement is the Wye connection, whereas secondary windings are connected in Wye and reversed Wye creating truly six phase system (phases spaced by 60 degrees).

5. The results of the real life model tests

The model of the MC and two six to three phase transformers were tested in the laboratory under following conditions:

- Input of the MC was supplied from the grid via a 230/48 V three to six phase transformers.
- Additional capacitors connected in Wye were connected at the MC input to create truly voltage source inverter (for all six phases).
- Switches were protected by snubber circuits.
- The resistive load was applied as six phase load connected in Wye.
- The reactive load was applied as three phase load supplied via six to three phase transformer and protected using varistors.

The main investigated property includes the potential of the practical application of the proposed control schemes. The tests were lead for all proposed controls and for resistive and reactive loads. The points of interests taken into account in this research include the commutation problems, the shape of the input and output current and voltage waveforms, the order of produced harmonics, *THD* and voltage transfer.

Due to the fact that the ‘as close as possible’ and ‘two closest’ strategies operate over the envelope of the waveform of input voltages (which is not a constant line), the output voltage can be created only from the voltages available at the input at the same instant. This fact causes the output voltage transfer to become a function of the input-output phase shift. For the ‘crossing point approach’, where output voltage waveforms are created only from parts of input sinusoids, which are crossing the desired output sinusoids, the voltage transfer is angle shift independent and is equal to the worst case for the ‘as close as possible’ control. For all strategies, if the number of input phases increases, the voltage transfer increases – this is associated with the size area closed by the envelope of the waveforms of the multiphase system.

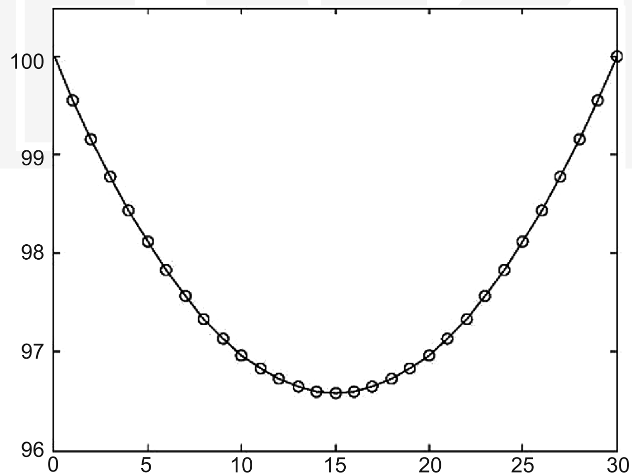

Fig. 16. Voltage transfer versus angle shift for ‘two closest’ control and 12×12 MC

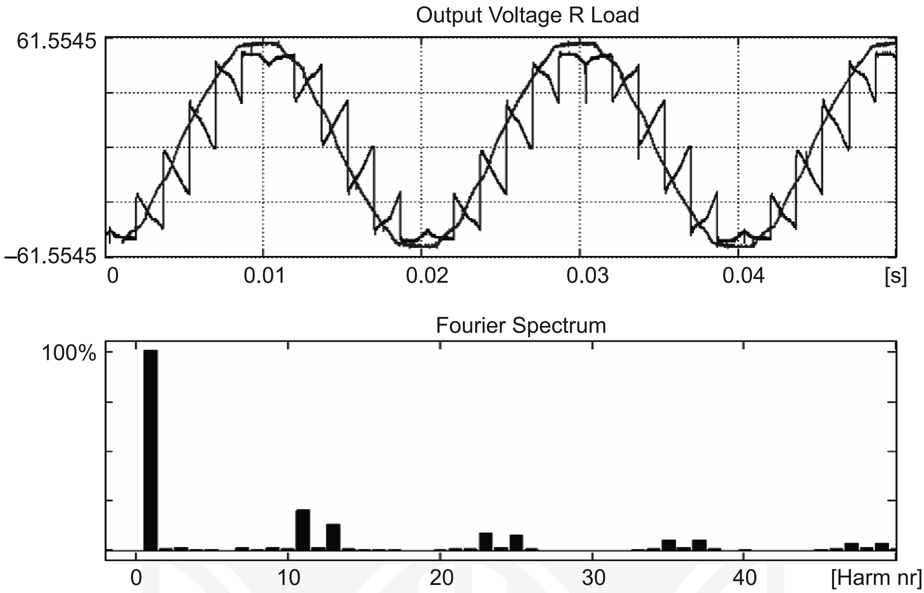

Fig. 17. Output voltage waveform versus input one and output *FFT* for the 'crossing point' approach resistive load and 10 degrees phase shift

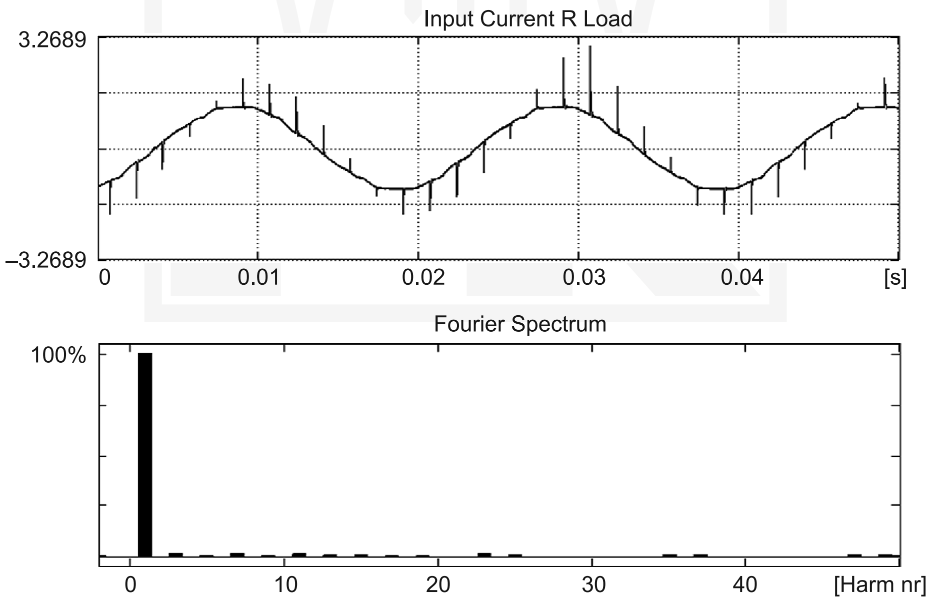

Fig. 18. Input current waveform and its *FFT* for the 'crossing point' approach resistive load and 10 degrees phase shift

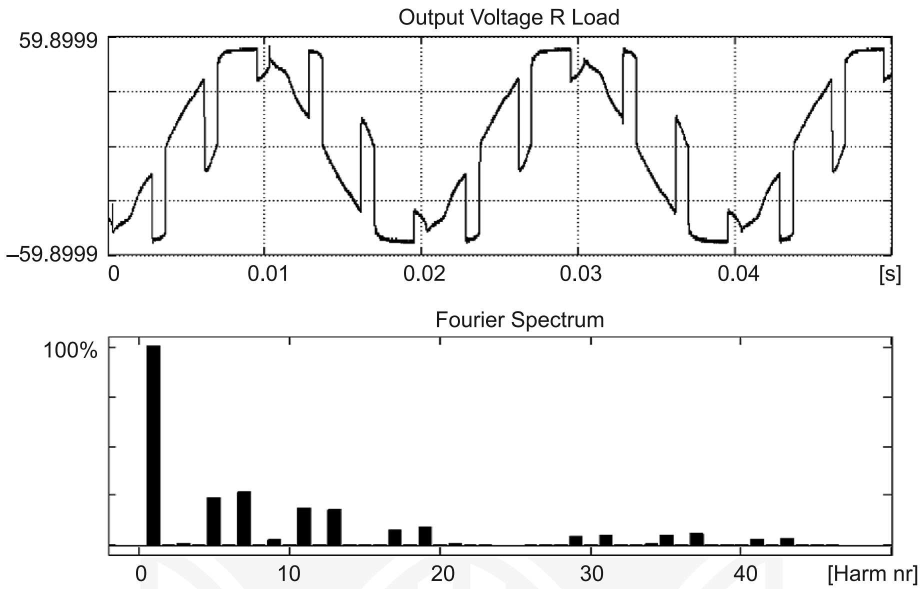

Fig. 19. Output voltage waveform and its *FFT* for the 'two closest' approach resistive load and 10 degrees phase shift

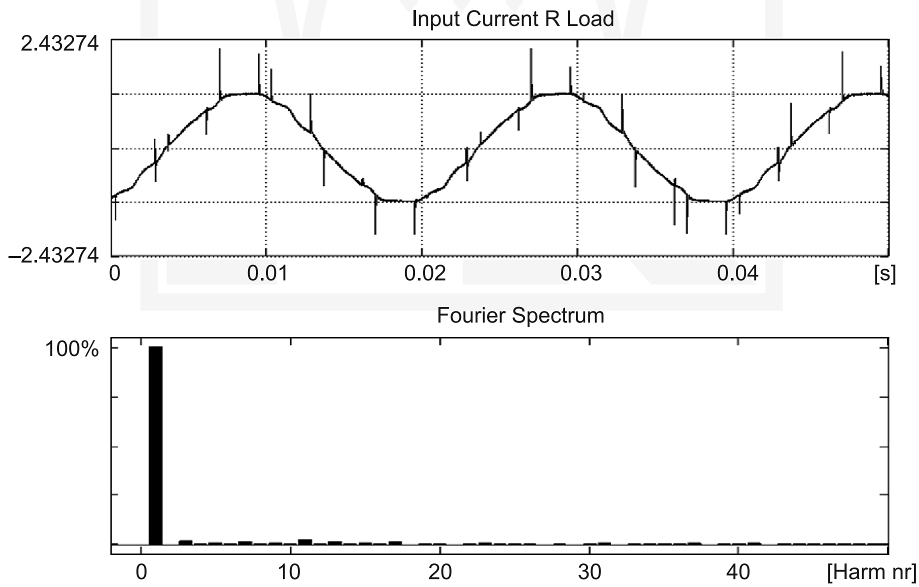

Fig. 20. Input current waveform and its *FFT* for the 'two closest' approach resistive load and 10 degrees phase shift

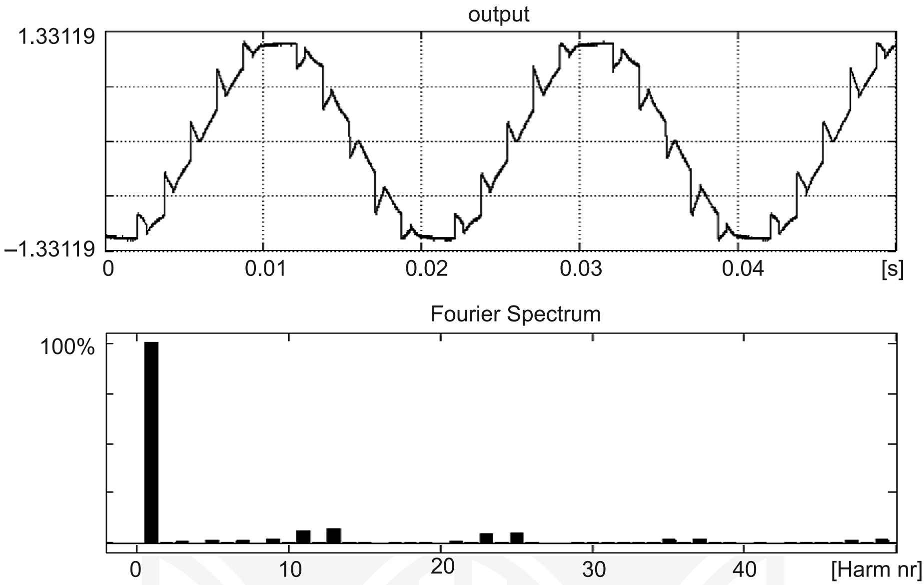

Fig. 21. Output voltage waveform and its *FFT* for the 'as close as possible' approach resistive load and 10 degrees phase shift

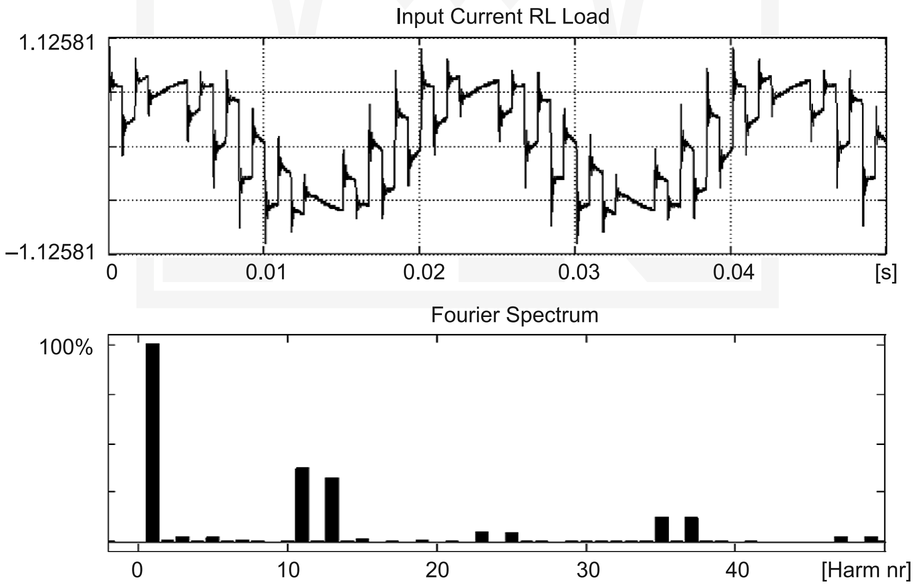

Fig. 22. Output voltage waveform and its *FFT* for the 'two closest' approach inductive load ($R = X$) and 10 degrees phase shift

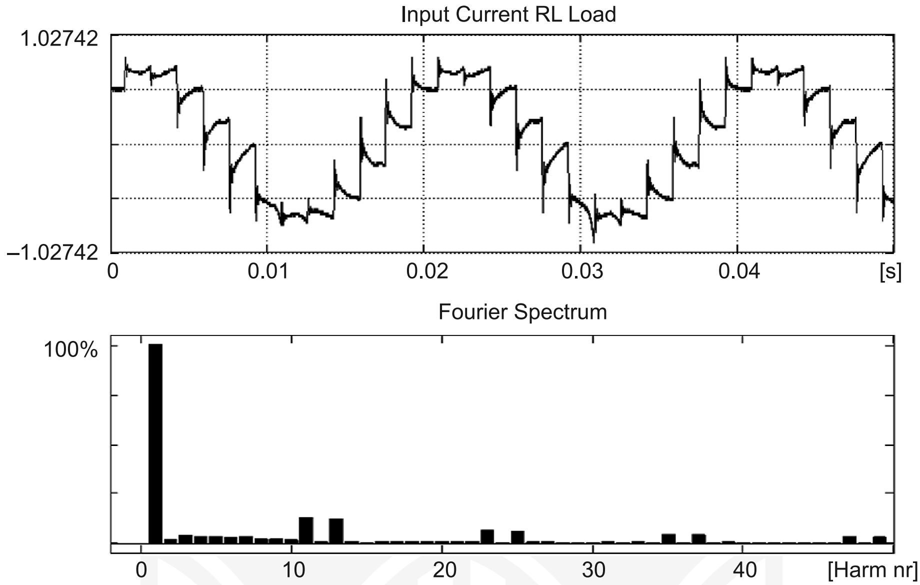

Fig. 23. Output voltage waveform and its *FFT* for the ‘crossing point’ approach inductive load and 10 degrees phase shift

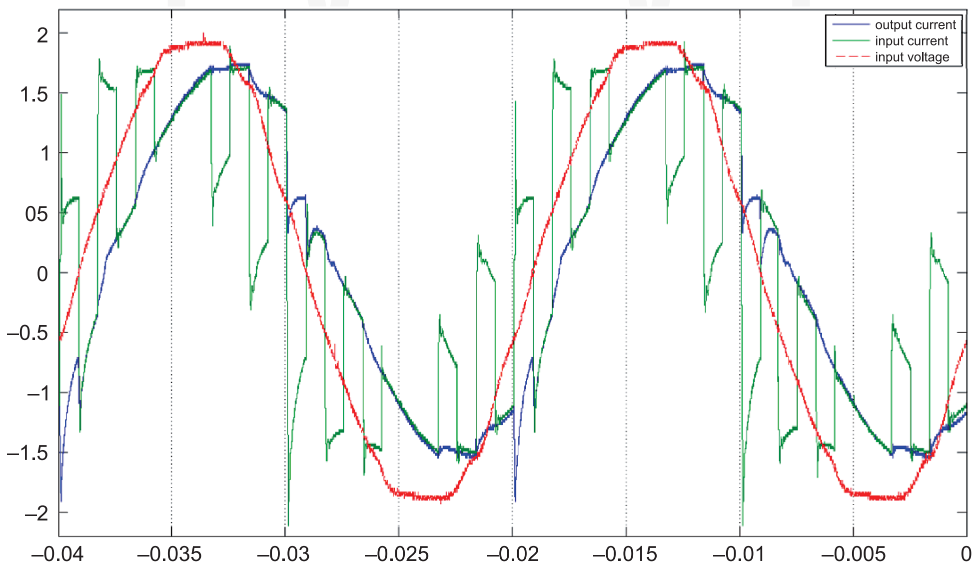

Fig. 24. Input voltage waveform (red) versus input (green) and output current (blue) for the ‘as close as possible’ approach inductive load and 12 degrees phase shift

The example of dependency of voltage transfer versus angle shift for ‘two closest’ control achieved by series of the consecutive simulations is shown in Fig. 16. The above figure shows only the 0 to 30 degrees range, since for the 12×12 MC situation repeats every 30 degrees. Similar curves can be obtained for the ‘as close as possible’ approach. For both control strategies, for the N phase system, minimum voltage transfer and maximum distortion occurs for $\pi/N+k\cdot 2\cdot\pi/N$ and maximum voltage transfer and minimum distortion for $k\cdot 2\cdot\pi/N$.

Figures 17 and 18 show output voltage and its *FFT* and input current and its *FFT* for resistive load for MC working under the ‘crossing point’ algorithm, Figs. 19 and 20 represent the same waveforms for the ‘two closest’ approach and Fig. 21 shows the output voltage for the ‘as close as possible’ approach.

Figures 22 and 23 present the output voltage of the converter for an inductive current and the ‘two closest’ and ‘crossing point’ approaches.

Figure 24 shows relative position of the input voltage and input and output currents for the ‘as close as possible’ approach. It is visible that as phase shift changes, the position of the first harmonic of the input current shifts with respect to the input voltage.

6. Conclusions

The tests performed in the laboratory using the real life model confirmed the results obtained during computer simulations. The proposed method of delivering the vectors of switches states, based on the developed memory search technique was found to be reliable and fast enough to use, even for a twice as dense digitalization of the conduction area (360×360 division was originally used). The matrix, built from proposed switches (28 A, 600 V rated IGBT and diodes) was found to be unexpectedly durable even in the case of overcurrents and overvoltage caused by operator errors.

The main problem noticed and investigated during laboratory research was associated with the commutation of the switches. The commutation problems were attributed to the type of the converter source and load. In the laboratory setup, the converter works from the voltage source (large capacitor bank) into the inductive load. For this setup, the considered commutation setup included the instantaneous change of the control signal for all switches, commutation delay characterized by introduction of ‘0’ state between the changes of control signal and commutation overlap where the switches already ‘on’ are kept ‘on’ for little longer while new set of switches is already turned ‘on’.

The first approach (instantaneous switching) was applied for laboratory setup and caused slight overcurrents at the input and overvoltages at the output. The second approach also applied in the lab caused overvoltages at the output and due to the speed of IGBT produced discontinuity of the currents. The commutation overlap was tested during simulation and in the lab for use when both sides of the converter had an inductive character to prevent overvoltages.

Due to a lack of funds, the MC has not yet been introduced into the power system to control the power flow, but an appropriate laboratory setup was already made.

Further research associated with the MC application in power systems will include the modification of the synchronization method, since methods based on the detection of input voltage were found to be unreliable and the application of the output synchronization for adaptation of the MC to work between systems with two different frequencies. The research has to include the evaluation of the MC dynamic properties which requires the adaptation of the control circuitry in order to be able to introduce step change into input signals (angle and frequency change).

Other directions of research should include the adaptation of the controller to make it able to create a controlled length of overlap during commutation in circuits with inductive elements on both sides of the converter or a controlled length of '0' state during commutation with a capacitive character on one side of the converter.

References

[1] Szczepanik J., Sieńko T., *Nowoczesne urządzenia do kontroli rozpływu mocy w systemie elektroenergetycznym oparte na wielofazowym przekształtniku macierzowym*, Zeszyty Naukowe Wydziału Elektrotechniki i Automatyki Politechniki Gdańskiej Nr 32, 2013, pp. 83-86.

[2] Szczepanik J., Sieńko T., *New Multiphase Matrix Converter Based Device for Power Flow Control*, Acta Energetica, 04/17 (2013), pp. 14-21, doi: 10.12736/issn.2300-3022.2013413.

[3] Empringham L., Kolar J.W., Rodriguez J., Wheeler P.W., Clare J.C., *Technological Issues and Industrial Application of Matrix Converters: A Review*, Industrial Electronics, IEEE Transactions on, vol. 60, no. 10, Oct. 2013, pp. 4260, 4271, doi: 10.1109/TIE.2012.2216231.

[4] Rodriguez J., Rivera M., Kolar J.W., Wheeler P.W., *A Review of Control and Modulation Methods for Matrix Converters, Industrial Electronics*, IEEE Transactions on, vol. 59, no. 1, Jan. 2012, pp. 58, 70, doi: 10.1109/TIE.2011.2165310.

[5] Kolar J.W., Friedli T., Rodriguez J., Wheeler P.W., *Review of Three-Phase PWM AC–AC Converter Topologies, Industrial Electronics*, IEEE Transactions on, vol. 58, no. 11, Nov. 2011, pp. 4988, 5006, doi: 10.1109/TIE.2011.2159353.

[6] Wheeler P.W., Rodriguez J., Clare J.C., Empringham L., Weinstein A., *Matrix converters: a technology review*, Industrial Electronics, IEEE Transactions on, vol. 49, no. 2, Apr. 2002, pp. 276, 288, doi: 10.1109/41.993260.

[7] Casadei D., Serra G., Tani A., Zarri L., *A review on matrix converters*, Przegląd Elektrotechniczny, vol. 82, nr 2, 2006, pp. 15-25, ISSN 0033-2097.

[8] Friedli Th., Kolar J.W., *Milestones in Matrix Converter Research*, IEEJ Journal of Industry Applications, vol. 1, 2012, pp. 2-14.

[9] Nguyen T.D., Hong-Hee Lee, *Dual Three-Phase Indirect Matrix Converter With Carrier-Based PWM Method*, Power Electronics, IEEE Transactions on, vol. 29, no. 2, Feb. 2014, pp. 569, 581, doi: 10.1109/TPEL.2013.2255067.

[10] Sun Y., Xiong W., Su M., Li X., Dan H., Yang J., *Topology and Modulation For a New Multi--Level Diode-Clamped Matrix Converter*, Power Electronics, IEEE Transactions on, vol. PP, no. 99, 2015, p. 1, doi: 10.1109/TPEL.2014.2305711.

[11] Keping You, Dan Xiao, Rahman M.F., Uddin M.N., *Applying Reduced General Direct Space Vector Modulation Approach of AC–AC Matrix Converter Theory to Achieve Direct Power Factor Controlled Three-Phase AC–DC Matrix Rectifier*, Industry Applications, IEEE Transactions on, vol. 50, no. 3, May–June 2014, 2243, 2257, doi: 10.1109/TIA.2013.2285956.

[12] Rivera M., Rojas C., Wilson A., Rodriguez J., Espinoza J., Baier C., Muñoz J., *Review of predictive control methods to improve the input current of an indirect matrix converter*, Power Electronics, IET, vol. 7, no. 4, April 2014, pp. 886, 894, doi: 10.1049/iet-pel.2013.0327.

[13] Nguyen T.D., Hong-Hee Lee, *A New SVM Method for an Indirect Matrix Converter With Common-Mode Voltage Reduction*, Industrial Informatics, IEEE Transactions on, vol. 10, no. 1, Feb. 2014, pp. 61, 72, doi: 10.1109/TII.2013.2255032.

[14] Dasika J.D., Saeedifard M., *A post-fault modulation strategy to control the matrix converter under an open-switch failure*, Applied Power Electronics Conference and Exposition (APEC), 2014 Twenty-Ninth Annual IEEE, 16–20 March 2014, pp. 1522, 1529, doi: 10.1109/APEC.2014.6803509.

[15] Laskody T., Prazenica M., Kascak S., *Space vector PWM for two-phase four-leg matrix converter*, ELEKTRO, 19–20 May 2014, pp. 324, 327, doi: 10.1109/ELEKTRO.2014.6848911.

[16] Dabour S.M., Rashad E.M., *A new continuous PWM strategy for three-phase direct matrix converter using indirect equivalent topology*, Power Electronics, Machines and Drives (PEMD 2014), 7th IET International Conference on 8–10 April 2014, pp. 1, 6, doi: 10.1049/cp.2014.0383.

[17] Garcia C., Rivera M., Lopez M., Rodriguez J., Pena R., Wheeler P., Espinoza J., *A Simple Current Control Strategy for a Four-Leg Indirect Matrix Converter*, Power Electronics, IEEE Transactions on, 2015, vol. PP, no. 99, p. 1, doi: 10.1109/TPEL.2014.2321562.

[18] Moin Ahmed SK., Abu-Rub H., Iqbal A., *Multiphase Matrix Converter Topologies and Control*, [in:] *Power Electronics for Renewable Energy Systems, Transportation and Industrial Applications*, eds. H. Abu-Rub, M. Malinowski, K. Al-Haddad, John Wiley & Sons, Ltd, Chichester, UK 2014, doi: 10.1002/9781118755525.ch15.

[19] Levi E., Bodo N., Dordevic O., Jones M., *Recent advances in power electronic converter control for multiphase drive systems*, Electrical Machines Design Control and Diagnosis (WEMDCD), 11–12 March 2013 IEEE Workshop on, pp. 158, 167, doi: 10.1109/WEMDCD.2013.6525176.

[20] Ahmed S.K.M., Iqbal A., Abu-Rub H., *Generalized Duty-Ratio-Based Pulsewidth Modulation Technique for a Three-to-k Phase Matrix Converter*, Industrial Electronics, IEEE Transactions on, vol. 58, no. 9, Sept. 2011, pp. 3925, 3937, doi: 10.1109/TIE.2010.2098373.

[21] Rahman K., Iqbal Am., Abduallah A.A., Al-ammari R., Abu-Rub H., *Space vector pulse width modulation scheme for three to seven phase direct matrix converter*, Applied Power Electronics Conference and Exposition (APEC), 16–20 March 2014 Twenty-Ninth Annual IEEE, pp. 595, 601, doi: 10.1109/APEC.2014.6803369.

[22] Bojoi R., Neacsu M.G., Tenconi A., *Analysis and survey of multi-phase power electronic converter topologies for the more electric aircraft applications*, Power Electronics, Electrical Drives, Automation and Motion (SPEEDAM), 20–22 June 2012 International Symposium on, pp. 440, 445, doi: 10.1109/SPEEDAM.2012.6264566.

[23] Ahmed Sk Moin, Abu-Rub Haitham, Salam Zainal, Iqbal Atif, *Dual matrix converters based seven-phase open-end winding drive*, Industrial Electronics (ISIE), 1–4 June 2014 IEEE, 23rd International Symposium on, pp. 2105, 2110, doi: 10.1109/ISIE.2014.6864942.

[24] Szczepanik J., Sienko T., *A new concept of application of multiphase matrix converter in power systems*, EUROCON, 2007, The International Conference on &# 34; Computer as a Tool&# 34; 1535-1540 2007 IEEE.

[25] Szczepanik J., Sienko T., *New control strategy for multiphase matrix converter*, Systems Engineering, 2008, ICSENG, 19th International Conference IEEE.

[26] Szczepanik J., Sienko T., *The Study of Implementation of Multiphase Matrix Converter in Power Systems*, Przegląd Elektrotechniczny, nr 89, 2013.

[27] Sieńko T., *Schemat zastępczy przekształtnika macierzowego dla stanów dynamicznych przy sterowaniu jednookresowym*, Czasopismo Techniczne, z. 1- E/2012, pp. 123-134.

[28] Sieńko T., Sobczyk T.J., *Modelling concept of N×M matrix converter under periodic control for dynamic states*, Archives of Electrical Engineering, vol. 63, no. 2, 2014, pp. 305-315.

[29] Sobczyk T.J., *Control strategy of matrix converters*, Proc. of European Conf. on Power Electronics and Applications (EPE), 1993, vol. 4, pp. 93-97.

[30] Sobczyk T.J., *The matrix converter – a universal power electronic unit*, Prace Instytutu Elektrotechniki, 2002, vol. 211, pp. 6-21.

[31] Sobczyk T., Szczepanik J., Rudek P., *Application of Matrix converter as an inter-connection device in the power system*, Czasopismo Techniczne, z. 3-E/2006, pp. 23-36.

[32] Sienko T., Szczepanik J., Sobczyk T.J., *Voltage phase controller for power systems*, Electrical Power Quality and Utilisation, 2007, EPQU, 9th International Conference on 1–6 2007, IEEE.

[33] Sobczyk T.J., Sienko T., *Application of matrix converter as a voltage phase controller in power systems*, Power Electronics, Electrical Drives, Automation and Motion, 2006, SPEEDAM, International Symposium on, IEEE, pp. 1322-1325.

[34] Sobczyk T.J., Sienko T., *Matrix converters control for high speed generators*, Electric Machines and Drives, 2005, IEEE International Conference on, IEEE, pp. 1975-1980.

[35] Sobczyk T.J., Sienko T., Danilewicz J.B., *Study of asymmetrical regimes in matrix converters for multi-phase high speed generators*, Power Tech, 2005, IEEE Russia, pp. 1-6.

[36] Sienko T., Sobczyk T., *Matrix converter control for applications to multi-phase high-speed microgenerators*, Archives of Electrical Engineering, vol. 53, no. 2, 2004, pp. 217-228, Polish Scientific Publishers.